5A halo of dark matter and neutron stars: relationship to gamma-ray bursts

A. V. Gurevich, V. S. Beskin, K. P. Zybin, and M. O. Ptitsyn

P. N. Lebedev Physics Institute, Russian Academy of Sciences
(Submitted 25 November 1992)
Zh. Eksp. Teor. Fiz. **103**, 1873–1890 (June 1993)

We predict the existence of an extensive halo of dark matter and fossil neutron stars reaching out to 300–400 kpc, and we find the spatial distribution of the latter. The suggestion that neutron stars are the source of gamma ray bursts is shown to be in good quantitative agreement with observational data. This model can be directly tested by investigating the angular anisotropy of observed gamma ray bursts.

1. INTRODUCTION

Gamma ray bursts—brief (1–10 sec) bursts of cosmic gamma emission—are presently an unresolved problem of astrophysics.[1-3] The basic problem is that they have yet to be identified with a single known cosmic source, and as a result, neither distances nor luminosities have been determined. Luminosity estimates based on the observed flux, $F \sim 10^{-5}$–10^{-7} erg/(cm^2 sec), depend heavily on the location of the sources: the implied energy release is 10^{37}–10^{38} erg for a distance of order 200 pc, or 10^{41}–10^{43} erg for distances 10–100 kpc. That much energy can only come from a stellar source. Other observational evidence, particularly the rapid ($\sim 10^{-3}$–10^{-4} sec) burst signal variability[4,5] and spectral features detected in the early experiments in the 10–30 keV range (the "cyclotron" line for a magnetic field $B \sim 10^{12}$ G) and in the 400–500 keV range ("annihilation" line, redshifted in a gravitational field), suggests that neutron stars are the sources of gamma ray bursts.[6-8]

At the same time, a statistical analysis of the observational data shows that the sources of gamma ray bursts are quite uniformly distributed over the celestial sphere, and are not concentrated toward the Galactic disk.[1-3] On the other hand, a log N–log S analysis of sources conclusively demonstrates that they are nonuniformly distributed in space: there is a significant preponderance of nearby sources (details can be found in Sec. 4). Statistical characteristics such as these probably only make sense if the sun is situated close to the center of an extensive, spherically symmetric cluster of sources whose density falls off markedly with distance from the center.[9,10]

Clearly, such a spatial distribution of sources might be associated with an extensive corona of neutron stars around the Milky Way,[11] but the nature of that corona remains completely unclear. The reason is that neutron stars born in the disk cannot travel much farther than 5–10 kpc,[12-14] i.e., much farther than the sun's distance $r_\odot \approx 8.5$ kpc from the center of the Galaxy, which leads to a source distribution inconsistent with the observations.

In the present paper, by analyzing the dynamics of dark matter during the time that Galactic structure was being formed, we show that an extensive halo of dark matter with $R_0 \approx 300$–400 kpc inevitably forms in the neighborhood of the Galaxy. This is also the size of the halo of fossil neutron stars that would have descended from the supernovae known to have initially enriched the interstellar medium with heavy elements.[15] As we shall see, this model provides not just a qualitative, but a quantitative explanation of the observed statistics of gamma ray bursts, and furthermore, it enables us to make detailed predictions about their energy budget. We are thereby able to map out a clear test path for this model, entailing direct comparison with observational data. If the theoretical predictions are not borne out, we will be able to affirm that neutron stars in the Milky Way are not the sources of gamma ray bursts.

2. FOSSIL NEUTRON STARS

It is well known that during the time of galaxy formation, primordial material consisting of hydrogen and helium was transformed into galactic gas, which in chemical terms has a high heavy-element abundance.[15] Matter was transformed during the early stages of protogalactic development as a result of the rapid contraction and burnout of massive stars, accompanied by supernova explosions. In addition, those explosions produced neutron stars[16] that we shall refer to as primordial or fossil neutron stars in order to distinguish them from those that result from processes taking place in the interstellar medium under conditions prevailing in already existing galaxies.

Dark matter plays a fundamental dynamical role in the early stages of protogalactic evolution. Newly formed neutron stars do not undergo collisions, so they move like dark matter. As a result, the distribution of fossil neutron stars (FNS) forms a halo, which hardly varies at all during the subsequent evolution of the galaxy. The basic characteristics of an FNS halo are therefore determined at birth, during the initial formation of a protogalaxy.

Note that the epoch at which a protogalaxy initially forms and its size are governed by the density of the dark matter contained within it. In fact, the epoch at which a self-contained clump of matter out of which a galaxy will eventually form comes together is notable in that the Hubble flow is curtailed within that clump—it can then be identified as an independent element in the universe. At that point, the Hubble flow merely increases the separation between clumps. Furthermore, as the universe expands, the mean density of dark matter decreases with time t as

$$\rho_d = \rho_0 (t_0/t)^2, \tag{1}$$

 1063-7761/93/060925-09$10.00

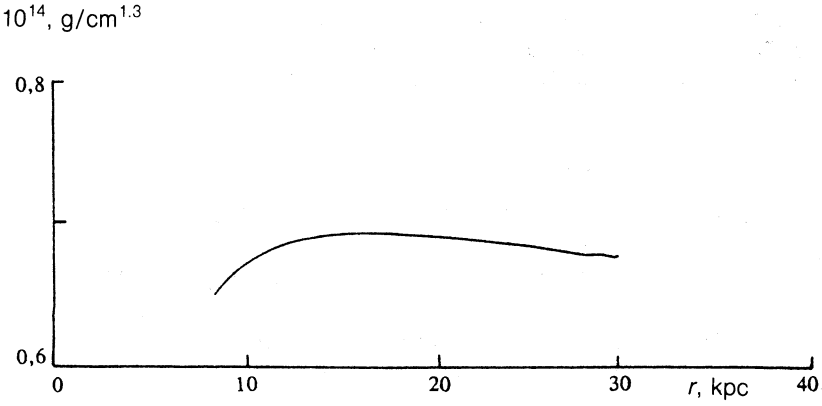

FIG. 1. The function $k(r)$ for the Milky Way.

where ρ_0 is the mean density of dark matter at the time of protogalaxy formation t_0. Within a clump of dark matter corresponding to a given galaxy, the density remains constant, which means that the density of dark matter within a given galaxy is fixed at the time of formation.

We assume that the stationary clumps of dark matter formed as a result of fragmentation are spherically symmetric, and have a density distribution[17]

$$\rho_d = kr^{-\alpha}, \quad \alpha \approx 1.7\text{–}1.8. \tag{2}$$

The total mass of dark matter contained within such a clump is therefore

$$m = \frac{4\pi}{3-\alpha} k R_0^{3-\alpha}, \tag{3}$$

where R_0 is the effective size of the clump, whereupon

$$R_0 = \left[\frac{(3-\alpha)m}{4\pi k}\right]^{1/(3-\alpha)} = \left[\frac{(3-\alpha)M_G}{4\pi k p}\right]^{1/(3-\alpha)}. \tag{4}$$

In Eq. (4), the mass of captured dark matter m is expressed in terms of the mass M_G of visible (baryon) matter in the galaxy and the parameter p, the ratio of baryon density to dark-matter density,

$$p = \frac{\rho_b}{\rho_d}. \tag{5}$$

Note that at the epoch of protogalaxy formation, baryon and dark matter are uniformly intermingled, so that p is a constant for all galaxies. Similarly, at the capture time t_0—the epoch of protogalaxy formation—we have

$$\begin{aligned} t_0 &= \frac{t}{(1+Z_0)^{3/2}}, \quad Z_0 = \frac{R_t}{R_0} - 1, \\ R_t &= \left(\frac{3}{4\pi}\frac{m}{\rho_{dt}}\right)^{1/3} = \left(\frac{3}{4\pi}\frac{M_G}{\rho_{bt}}\right)^{1/3}. \end{aligned} \tag{6}$$

Here ρ_{bt} and ρ_{dt} are the mean baryon and dark-matter density in the universe at the present time t, and R_t is the effective distance between galaxies.

It is important that we be able to determine k for each galaxy via the observed rotation curve $V(r)$. Using the virial theorem[18] and Eq. (2), we have

$$V^2 = (2-\alpha)\Psi = \frac{4\pi}{3-\alpha} k G r^{2-\alpha}, \tag{7}$$

and therefore

$$k = \frac{3-\alpha}{4\pi} \frac{V^2(r)}{G r^{2-\alpha}}.$$

We have plotted $k(r)$ in Fig. 1 for the Milky Way, taking $\alpha = 1.7$. We see that beyond 8–10 kpc, where dark matter begins to predominate, $k(r)$ will be almost constant:

$$\left.\begin{aligned} k &= 0.7 \cdot 10^{14} r^{1.3}, \quad \alpha = 1.7, \\ k &= 1.2 \cdot 10^{16} r^{1.2}, \quad \alpha = 1.8, \end{aligned}\right\} r \text{ in cm}. \tag{8}$$

This value is in good agreement with the density of dark matter usually assumed for the solar neighborhood,[19] $\rho_d(r_\odot) = 0.3\text{–}0.4$ GeV/cm^3, since (2) and (8) imply that for $\alpha = 1.7$

$$\rho_d(r_\odot) = k r_\odot^{-\alpha} = 0.56 \cdot 10^{-24} \text{ g/cm}^3 \approx 0.31 \text{ GeV/cm}^3.$$

Knowing k, we can then determine R_0 and Z_0:

$$R_0 = R_h \left(\frac{3\%}{p} \frac{M_G}{3 \cdot 10^{44} \text{ g}}\right)^{1/(3-\alpha)}, \tag{9}$$

$$Z_0 = Z_h \left(\frac{p}{3\%}\right)^{1/(3-\alpha)} \left(\frac{3 \cdot 10^{44} \text{ g}}{M_G}\right)^{\alpha/(9-3\alpha)} - 1, \tag{10}$$

where $R_h = 310$ kpc, $Z_h = 6.8$ for $\alpha = 1.7$ and $R_h = 440$ kpc, $Z_h = 4.8$ for $\alpha = 1.8$.

Thus, for each galaxy, the size R_0 of the primordial clump and the epoch Z_0 at which it first appears can be expressed in terms of the observable quantity k, the mass of the galaxy M_G, and the parameter p, which is the same for all galaxies. Note that p actually varies over a small range. In fact, if we assume that the universe is marginally closed ($\Omega \approx 1$), then p will be directly related to the Hubble constant H:

$$p = \frac{8\pi}{3} \frac{G\rho_b}{H^2}.$$

Thus, taking $\rho_b \approx 3 \cdot 10^{-31}$ g/cm^3, the range of variation of p is

$$2\% < p < 7.5\% \text{ for } 50 < H < 100 \text{ km/sec} \cdot \text{Mpc}. \tag{11}$$

The distribution of baryon gas in a primordial clump is the same as the distribution of dark matter (see Ref. 20). The density of primordial neutron stars should have a similar distribution,

$$n_1(r)=k_n r^{-\alpha}, \quad \alpha=1.7\text{–}1.8. \tag{12}$$

Here k_n is the fraction of all matter residing in neutron stars after the explosion of the primordial supernovae (PSN). Since the latter have masses[15,16]

$$M\sim(10\text{–}100)M_\odot, \tag{13}$$

while the mass of a neutron star is $M_n\approx 1.4M_\odot$, the mass tied up in fossil neutron stars should be from 1–2 to 10–20% of all stellar matter in the Galaxy.

This estimate naturally rests on a number of modeling assumptions. Foremost among these is that to determine k_n accurately, the mass distribution of primordial stars must be known; in general, it differs from the mass distribution of main-sequence stars.[15] The contribution of low-mass stars can thus reduce the estimated value of k_n. On the other hand, during the primordial galactic stage, i.e., close to the epoch of self-containment, there may be several populations of fossil neutron stars, rather than just one—a circumstance that can raise the estimate of k_n. It is conceivable, therefore, that the foregoing estimate of the ratio of neutron-star matter to baryon matter is a reasonable one.

Integrating (12) over the entire halo of FNS, we therefore obtain

$$k_n=\frac{3-\alpha}{4\pi}R_0^{\alpha-3}p_1N_G, \quad 0.01\text{–}0.02<p_1<0.1\text{–}0.2. \tag{14}$$

Here N_G is the total number of stars in the Galaxy, and p_1 is the fraction of all such stars that are fossil neutron stars.

Note that since the distribution of matter is already quite inhomogeneous by the time primordial supernovae start exploding, the mean mass of supernovae (11) and the implied number density of neutron stars may in fact vary with r. We can allow for this by allowing the parameter p_1 in (12) to depend on r:

$$p_1(r)=p_n(r/R_0)^{\varepsilon}, \tag{15}$$

where of course ε is small,

$$0<\varepsilon\ll\alpha, \tag{16}$$

so that the distribution of neutron stars is consistent with (2) and (12) overall.

An FNS halo formed about the Milky Way at birth should therefore have the following properties:

1) it should be spherically symmetric about the center of the Galaxy;

2) it should have size R_0 given by (9) at time Z_0 given by (10);

3) neutron stars should be distributed in radius as given by (12)–(16):

$$n_1(r)=p_n\frac{3-\alpha}{4\pi R_0^3}N_G\left(\frac{r}{R_0}\right)^{-\alpha+\varepsilon}. \tag{17}$$

The FNS distribution in the halo is thus specified by three parameters, p, p_n, and ε, which have small feasible ranges of variation given by (11), (14), and (16).

3. DISK NEUTRON STARS

We now consider neutron stars produced by processes in a galactic disk. Because of their high space velocities, these stars eventually leave the disk, forming the second component of the neutron star halo. That part of the halo population has already been studied a number of times.[12–14] But more often than not, the neutron stars' initial velocity distribution function has been assumed to be isotropic, while in reality the streaming motion associated with the general rotation of a galactic disk induces velocities much larger than the peculiar velocities of the neutron stars themselves, so that their actual motion is far from isotropic. Furthermore, in all previous papers, the model gravitational potential contained no explicit contribution attributable to dark matter [Eqs. (2), (8)].

We therefore consider the distribution of neutron stars spawned in a galactic disk, which we shall characterize by the distribution function $n_2(\mathbf{r},\mathbf{v},t)$, which must satisfy the kinetic equation

$$\frac{\partial n_2}{\partial t}+\mathbf{v}\frac{\partial n_2}{\partial \mathbf{r}}+\mathbf{a}\frac{\partial n_2}{\partial \mathbf{v}}=q(\mathbf{r},\mathbf{v}),$$

where $\mathbf{a}=d\mathbf{v}/dt$, and the function $q(\mathbf{r},\mathbf{v})$ describes the birth of neutron stars. Neutron stars are known to spend the first several million years of their lives (i.e., a much shorter time than the oscillation period in the Galactic gravitational field) as radio pulsars,[21,22] and besides their positions, we actually know the velocity $\mathbf{v}$ of many pulsars. We can therefore determine $q(\mathbf{r},\mathbf{v})$ directly from observations.

It is important to note that the halfwidth of the disk of observed pulsars is only $z_p\approx 100$ pc,[21,22] close to the halfwidth for supernova remnants ($z_{SN}\approx 60$ pc), which are closely related to the processes responsible for the formation of the disk neutron stars. As we shall see, the characteristic size of the cloud of old disk neutron stars is much larger than z_{SN}, so we can confidently assume that all disk neutron stars were born in a thin layer near $z=0$, i.e., $q(\mathbf{r},\mathbf{v})\propto\delta(z)$. It is also natural to assume that the (cylindrical) radial dependence of $q(\mathbf{r},\mathbf{v})$ is proportional to the density $n_0(\rho)$ of stars in the galactic disk, which is closely approximated by

$$n_0(\rho)=\frac{1}{\rho_G^2}\exp\left(-\frac{\rho}{\rho_G}\right), \tag{18}$$

where $\rho_G=4.5$ kpc.[15]

In turn, the observed space velocities of radio pulsars with respect to the sun enable us to determine how the source function $q(\mathbf{r},\mathbf{v})$ depends on velocity $\mathbf{v}$. Both interferometry[23] and scintillation[24] studies of transverse pulsar velocities indicate a decreasing distribution function with characteristic width $v_\perp\approx 70$–100 km/sec. Such a two-dimensional distribution corresponds to a distribution function

$$q_0(\mathbf{v}_r) \propto q_p \exp\left(-\frac{v_r^2}{2v_0^2}\right), \tag{19}$$

where $q_p \approx 1/30\ \mathrm{yr}^{-1}$ is the pulsar birthrate in the Galactic disk,[21,22] $\mathbf{v}_r$ is the neutron star velocity with respect to the sun, and $v_0 = v_\perp/\sqrt{2} \approx 50$–$70$ km/sec.

Note that radio interferometry indicates that there is also a second maximum at high velocities, $v_\perp \approx 300$ km/sec.[23] These data have not been confirmed by scintillation measurements, however, so they are not yet deemed completely reliable. For example, the distances to three high-velocity pulsars, PSR 0523+11, 0559−05, and 2148 +63, have been grossly overestimated, resulting in significant overestimates of their velocities (see Ref. 25). It is therefore natural that we confine our deliberations to the unimodal distribution function defined by (19). Although radio pulsar space velocities with respect to the sun are then greater than the space velocities of ordinary stars, they are nevertheless much lower than Galactic orbital velocities $V_0(\mathbf{r})$. To zeroth order in the small parameter $\mu = v_0/V_0(\mathbf{r})$, we can therefore neglect any perturbation to the orbital motion of a neutron star; in other words, we can assume that in cylindrical coordinates ρ and φ, they move with angular velocity $\Omega_0(\rho) = V(\rho)/\rho$, just like their parent supernovae. In that approximation, we can write the distribution in the form

$$n_2(\mathbf{r},\mathbf{v},t) = \frac{1}{2\pi} n_0(\rho) n_z(z,v_z,t) \delta(v_\rho) \delta(v_\varphi - V_0), \tag{20}$$

where the distribution function $n_z(z,v_z,t)$ must satisfy the kinetic equation

$$\frac{\partial n_z}{\partial t} + v_z \frac{\partial n_z}{\partial z} + a_z \frac{\partial n_z}{\partial v_z} = q_0(v_z)\delta(z)\theta(t). \tag{21}$$

Here a_z is the acceleration of the neutron star perpendicular to the Galactic disk.

The characteristic oscillation time of neutron stars relative to the Galactic plane is $\tau_0 \sim \Omega_0^{-1} \sim 300$–$500$ million years, which is much less than the Galactic evolution time $t_G \approx 6$–8 billion years, so it is safe to assume that they move in a stationary gravitational field. The acceleration can then be written as the gradient of a scalar potential, $a_z = -\nabla\Phi$, where

$$\Phi = \frac{\Omega_0^2(\rho) z^2}{2} + g(\rho)|z|. \tag{22}$$

Here

$$g(\rho) = 2\pi G M_d n_0(\rho), \tag{23}$$

and $M \approx 8 \cdot 10^{10}\ M_\odot$ is the mass of the Galactic disk component.[15] The first term in (22) then corresponds to the spherically symmetric potential (2) induced by dark matter, and the second, to the gravitational field of a thin disk. The resulting neutron star motion given by the kinetic equation (21) has an energy integral

$$E = \frac{v_z^2}{2} + \frac{\Omega_0^2(\rho) z^2}{2} + g(\rho)|z|, \tag{24}$$

where ρ here can be treated as a parameter. Finally, if we write out the density as

$$n_z(z,v_z,t) = N_z(z,t) q_0(E), \tag{25}$$

where we assume a source distribution function of the form

$$q_0(E) = \frac{(2E)^{1/2}}{2v_0^2} \exp\left(-\frac{E}{v_0^2}\right), \tag{26}$$

we finally reduce the continuity equation (21) to

$$\frac{\partial N_z}{\partial t} + v(z,E) \frac{\partial N_z}{\partial z} = \frac{1}{2}\delta(z)\theta(t). \tag{27}$$

Here

$$v(z,E) = [2E - \Omega_0^2(\rho) z^2 - 2g(\rho)|z|]^{1/2} \tag{28}$$

can be determined from the energy integral (24), and the factor 1/2 indicates that only half the neutron stars emerge from the Galactic disk with $z > 0$.

Equation (27) can easily be solved. Prior to the first reflection, for $t < T/4$, where $T(E)$ is the period of oscillation through the Galactic disk,

$$T(E) = 4 \int_0^{z_{\max}(E)} \frac{dz}{v(z,E)} \tag{29}$$

[$z_{\max}(E)$ is a turning point, at which $v(z_{\max},E) = 0$], we obtain

$$N_z(E,z,t) = \frac{1}{2v(0,E)} \left\{\theta(z) - \theta\left[t - \int \frac{dz}{v(z,E)}\right]\right\}, \quad z \geqslant 0.$$

For the more interesting case $t \gg T$, where the neutron stars manage to complete many trips through the Galactic plane, we have

$$n_z(z,v_z,t) = \frac{2q_0[E(z,v_z)]}{v[0,E(z,v_z)]} \frac{t}{T[E(z,v_z)]}. \tag{30}$$

As might have been expected, the neutron star density then grows linearly with the age t of the Galaxy. Finally, making use of (24)–(26) and (29), and integrating the distribution function (30) over velocity v_z, we ultimately obtain for the density of disk neutron stars

$$n_2(\rho,\varphi,z) = \frac{t_G q_p}{4\pi} \frac{n_0(\rho)}{z_0(\rho)} \exp\left[-\frac{z^2}{2z_0^2(\rho)} - \delta_1(\rho)\frac{z}{z_0(\rho)}\right] I(z,\rho),$$

$$I(z,\rho) = \int_0^\infty dx \exp\left(-\frac{x^2}{2}\right) \frac{1}{\frac{\pi}{2} - \arcsin\left\{\frac{\delta_1(\rho)}{x^2 + z^2/z_0^2(\rho) + 2\delta_1(\rho) z/z_0(\rho) + \delta_1^2(\rho)}\right\}^{1/2}}. \tag{31}$$

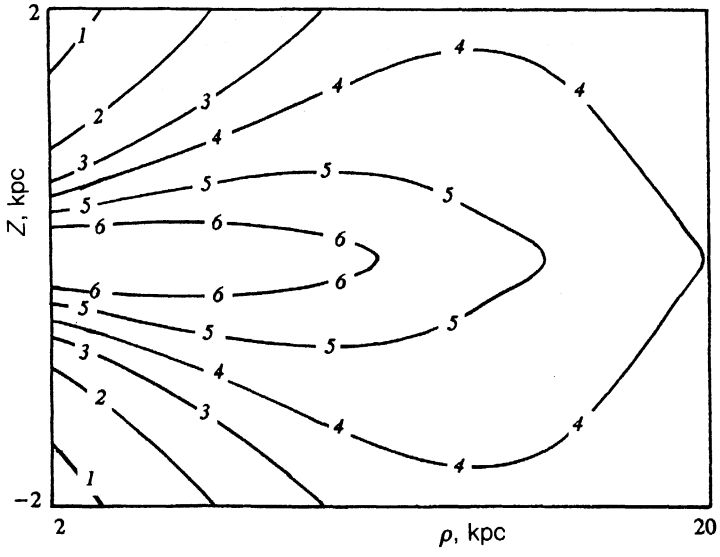

FIG. 2. Constant-density contours of $n_2(r)$ for disk neutron stars, $v_0=50$ km/sec. Log densities are *1*) 1.75, *2*) 2.50, *3*) 3.25, *4*) 4.00, *5*) 4.75, and *6*) 5.50, where the densities are measured in kpc^{-3}.

The dimensionless quantity

$$\delta_1(\rho)=\frac{2\pi GM_G n_0(\rho)}{\Omega_0(\rho)v_0}=70\left(\frac{\rho}{r_\odot}\right)^{0.85}\exp\left(-\frac{\rho}{\rho_G}\right)v_{50}^{-1} \quad (32)$$

in (31) specifies the importance of the disk gravitational field relative to the gravitational field due to dark matter, and

$$z_0(\rho)=v_0/\Omega_0(\rho)=0.23r_\odot(\rho/r_\odot)^{0.85}v_{50},$$
$$v_{50}=v_0/(50\ \text{km/sec}) \quad (33)$$

is in fact the thickness of the cloud of disk neutron stars as a function of the radial coordinate ρ. For the numerical estimates in Eqs. (32) and (33), we have utilized the explicit expressions (2) and (8) for the density of dark matter.

In Fig. 2, we have plotted contours of constant density for disk neutron stars, as given by Eqs. (31)–(33). We see that the characteristic thickness z_0 of the neutron star cloud at $r_\odot=8.5$ kpc from the Galactic center is approximately 1 kpc. The neutron stars in fact occupy part of a torus, with a substantial shortfall near the rotation axis for $z\neq 0$. This is as it should be, since neutron stars born in the vicinity of the Galactic center are located in a deep potential well, and are in no position to overcome the Galactic gravitational field. The total number of neutron stars in the disk, $N_2=t_G q_p$, is then $(1\text{–}2)\cdot 10^8$. Note that Prokhorov and Postnov[26] independently derived a toroidal distribution of disk neutron stars, but they did so using a different form for the gravitational potential.

4. COMPARISON WITH GAMMA RAY BURST OBSERVATIONS

We now assume that neutron stars are the sources of gamma ray bursts. Let a neutron star located at $\mathbf{r}$ emit a burst of radiation releasing total energy Q with probability $P(Q)$. An observer situated at $\mathbf{r}_0$ will record a total flux

$$S=\frac{Q}{4\pi R^2}, \quad R=|\mathbf{r}-\mathbf{r}_0|. \quad (34)$$

For simplicity, we will assume here that the radiation is isotropic. It is important that the sensitivity of the observer's equipment be limited—that bursts be detected only if the photon count rate C per unit time Δt exceeds a threshold level C_{lim}.[27] Accordingly, if we also assume that gamma ray bursts all have similar temporal profiles, we obtain the detection condition

$$S\geqslant S_{\min}. \quad (35)$$

In addition to the intensity, the observer will also identify a direction of arrival, given by Galactic coordinates l and b (see Fig. 3). In the present case, the observer is located a distance $r_\odot=8.5$ kpc from the Galactic center. Clearly, the rate of observed bursts will have some distribution $F(S,l,b)$ over flux S and the angles l and b, which we can characterize by certain mean values. With a view toward comparison with observations, we choose the mean parameters

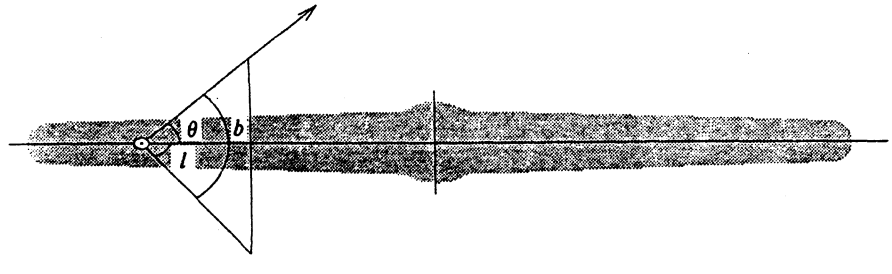

FIG. 3. Galactic coordinates l and b, with the sun's position in the Galaxy marked. The angle θ is reckoned from the direction of the Galactic center.

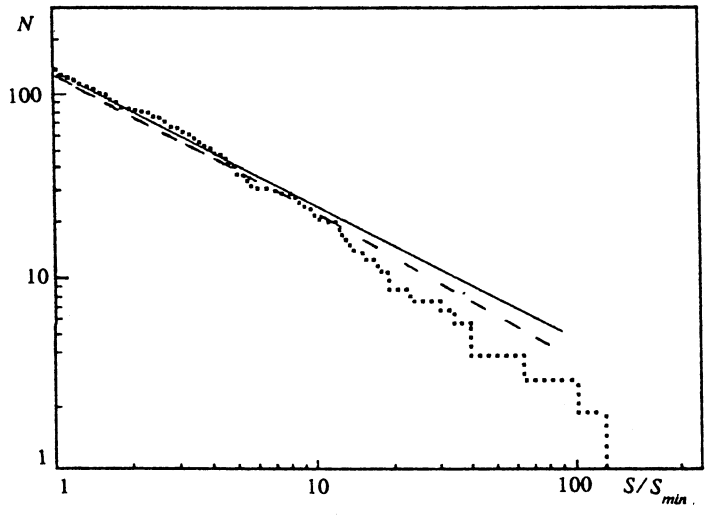

FIG. 4. Plot of log N vs log S as modeled by Eqs. (40)–(42). The continuous line corresponds to a "standard candle" model, the dashed line to a broad spectrum (42). The dots show the observed dependence, taken from Ref. 29.

$$\left\langle \frac{V}{V_{\max}} \right\rangle = \left\langle \left(\frac{S}{S_{\max}} \right)^{-3/2} \right\rangle = \frac{1}{N} \int_{S_{\min}} \left(\frac{S}{S_{\min}} \right)^{-3/2} F(S,l,b)\,dS\,dl\,db, \quad (36)$$

$$\langle \cos\theta \rangle = \frac{1}{N} \int_{S_{\min}} \cos l \cos b F(S,l,b)\,dS\,dl\,db, \quad (37)$$

$$\langle \sin^2 b \rangle = \frac{1}{N} \int_{S_{\min}} \sin^2 b F(S,l,b)\,dS\,dl\,db. \quad (38)$$

Here θ is the apparent angle between the source and the Galactic center (Fig. 3),

$$F(S,l,b) = \int n(\mathbf{r}) P(4\pi R^2 S) \cdot 4\pi R^2 dR \quad (39)$$

is the observed source distribution on the celestial sphere as a function of flux S, the argument of the probability function $P(Q)$ is defined by (34), and $n(\mathbf{r})$ is the density of neutron stars as a function of $\mathbf{r}$. Finally,

$$N = N(S_{\min}) = \int_{S_{\min}} F(S,l,b)\,dS\,dl\,db \quad (40)$$

is the total number of sources with flux greater than $S_{\min}$.

The quantity $\langle V/V_{\max} \rangle$ is essentially the number of sources in the more distant half of the observed volume, relative to the total number of observed sources.[27] For a spatially uniform distribution, $\langle V/V_{\max} \rangle = 1/2$. If on the other hand the number of sources $n(R)$ falls with distance as R^{-1}, then $\langle V/V_{\max} \rangle = 2/5$. Likewise, for $n(R) \propto R^{-2}$ we have $\langle V/V_{\max} \rangle = 1/4$. For a more detailed analysis of the spatial distribution of sources, we can turn to the

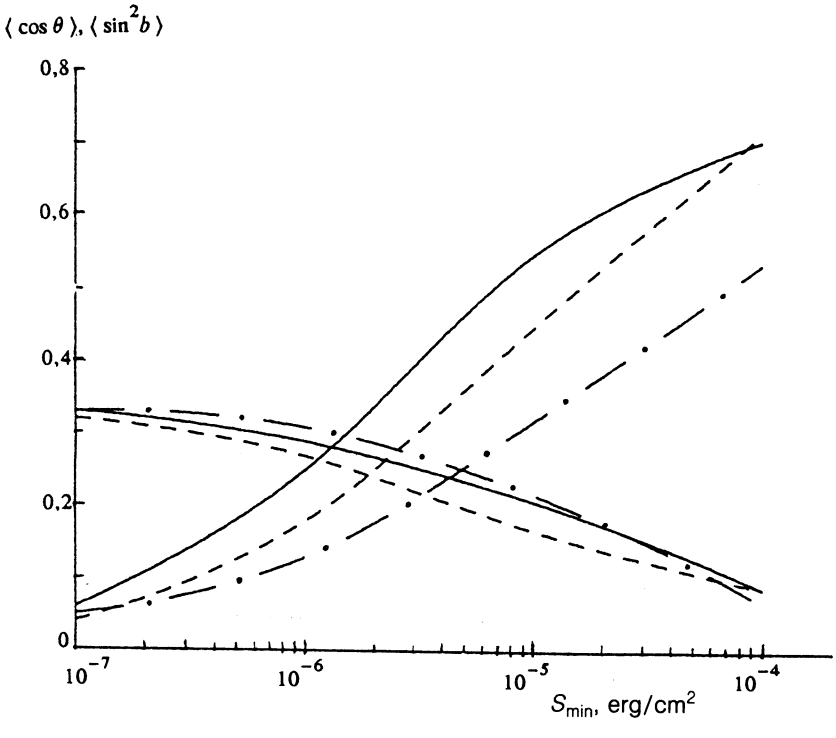

FIG. 5. Angular anisotropy $\langle \cos\theta \rangle$ and $\langle \sin^2 b \rangle$ as a function of threshold sensitivity $S_{\min}$. The continuous curves correspond to a "standard candle" (41), the dashed curves to (42), and the long-dash curves show the behavior for a "cutoff" distribution with $n_1(r) = n_1(r_c)$ at $r < r_c = 20$ kpc for a broad source function (42).

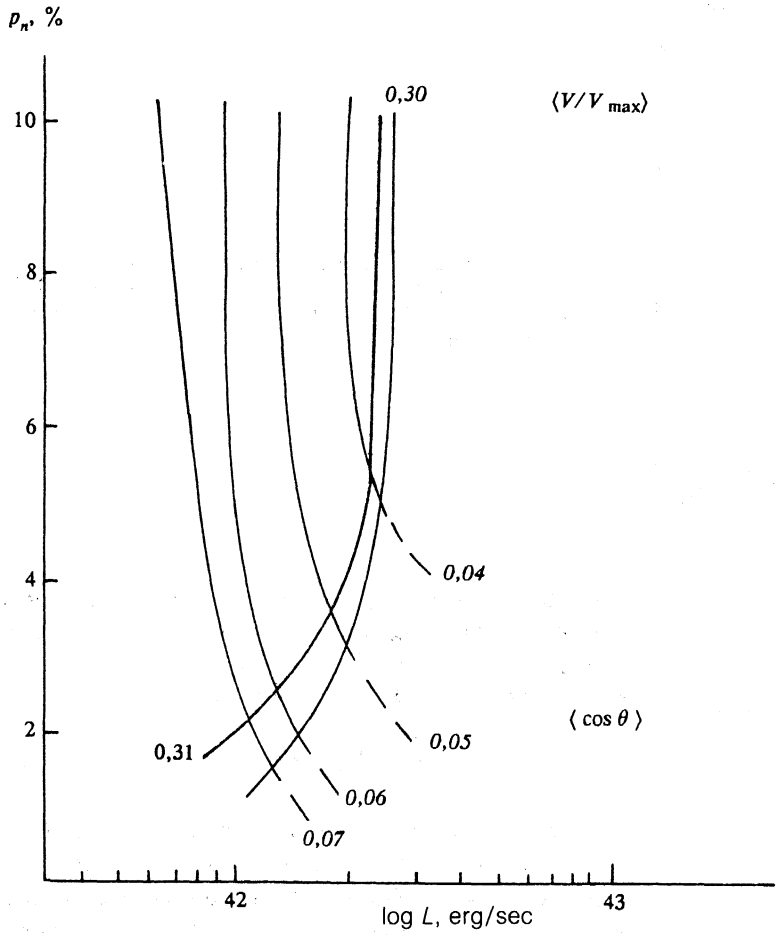

FIG. 6. Parameters $\langle V/V_{max}\rangle$ and $\langle \cos\theta\rangle$ as functions of the luminosity L and of the relative number of FNS compared to luminous matter p_n for $p=3\%$.

log N–log S plot, which shows how the number of observed sources declines as the threshold S_{min} increases (see Fig. 4).

Figures 4 and 5 show the results of calculations based on (17), (31), and (36)–(40). Figure 4, in particular, shows log N vs log S as obtained directly from (40). The straight line is what we would obtain for a "standard candle," where all sources have the same power, so that

$$P(Q)=\delta(Q-Q_0). \tag{41}$$

The dotted line corresponds to the broad distribution

$$P(Q)=\frac{1}{2.7Q_0},\quad 0.3Q_0<Q<3Q_0. \tag{42}$$

The log N–log S plot is clearly insensitive to the source distribution as a function of power (see, e.g., Ref. 10), so we will restrict our discussion principally to the distribution given by (41). On the other hand, the angular characteristics $\langle\cos\theta\rangle$ given by (37) and $\langle\sin^2 b\rangle$ given by (38) do depend critically on the total energy release Q and the sensitivity S_{min} (see Fig. 5).

Note that to estimate $\langle V/V_{max}\rangle$ and $\langle\cos\theta\rangle$ for $S\gtrsim S_{min}$, we can make use of the asymptotic behavior of the FNS density given by (17). In the limit $r_\odot/R_{max}\ll 1$, where

$$R_{max}=\left(\frac{Q}{4\pi S_{min}}\right)^{1/2} \tag{43}$$

(but of course $R_{max}<R_0$), we obtain the simple analytic results

$$\left\langle\frac{V}{V_{max}}\right\rangle=\frac{3-\alpha_{eff}}{6-\alpha_{eff}}, \tag{44}$$

$$\langle\cos\theta\rangle=\frac{\alpha_{eff}}{3}\frac{(3-\alpha_{eff})}{(2-\alpha_{eff})}\frac{r_\odot}{R_{max}}, \tag{45}$$

where $\alpha_{eff}=\alpha-\varepsilon$ is the power-law exponent in (17). If in fact $R_{max}>R_0$, there is an abrupt drop in $\langle V/V_{max}\rangle$, since most sources reside in the inner part of the observed volume.

We thus see that the asymptotic value of $\langle V/V_{max}\rangle$ actually depends solely on $\alpha_{eff}=\alpha-\varepsilon$. For $\alpha=1.7$ [see (12)] and $\varepsilon=0.1$ [see (16)], we obtain

$$\langle V/V_{max}\rangle=0.32. \tag{46}$$

Furthermore, substituting $\alpha_{eff}=1.6$ into (45) for $\langle\cos\theta\rangle$, we obtain

$$\langle\cos\theta\rangle=1.9\frac{r_\odot}{R_{max}}. \tag{47}$$

Accordingly, given a threshold $S_{min}=10^{-7}$ erg/cm^2 and energy distribution (41), we have

$$\langle\cos\theta\rangle=0.04(Q/2\cdot 10^{42}\ \text{erg/sec})^{-1/2}. \tag{48}$$

The analytic expressions (46)–(48) are in good agreement with the numerical results plotted in Figs. 4 and 5.

We can now compare the theoretical predictions with observations. The most recent data from the Compton Gamma-Ray Observatory, based on 426 sources,[28] yield

$$\langle V/V_{\max}\rangle = 0.32 \pm 0.02,$$
$$\langle \cos\theta\rangle = 0.04 \pm 0.03, \qquad (49)$$
$$\langle \sin^2 b\rangle = 0.32 \pm 0.01.$$

We thus see, as we pointed out in the Introduction, that the distribution of gamma ray bursts is highly isotropic, but spatially quite nonuniform. The agreement with our model is very good. In fact, since the total number of FNS,

$$N_1 = p_n N_G \approx 2 \cdot 10^{10}\left(\frac{p_n}{10\%}\right)$$

is much greater than the number of disk neutron stars

$$N_2 = t_G q_p \approx (1\text{–}2)\cdot 10^8,$$

while the radius (9) of the region occupied by FNS, $R_0 \approx 400$ kpc, is much greater than the sun's distance from the center of the Galaxy, $r_\odot = 8.5$ kpc, it is no wonder that the distribution of observed gamma ray bursts is both isotropic and spatially nonuniform (assuming them to be associated with neutron stars), since the sun would appear to be located almost at the center of an extended halo whose density (17) decreases rapidly with distance. Equation (47) then shows immediately that for isotropy to obtain [see (49)], the size $R_{\max}$ of the observed region must be quite large:

$$R_{\max} \simeq R_0 \simeq 300\text{–}400 \text{ kpc}.$$

This theory actually makes it possible to obtain quantitative agreement with the observations as well. In Figs. 6 and 7, we show the range of $\langle V/V_{\max}\rangle$ and $\langle \cos\theta\rangle$ in the $p_n - L$ plane for the two values $p = 3$ and 5% and a threshold sensitivity of $F = 10^{-7}$ erg/(cm$^2\cdot$sec), which is just the sensitivity of the Compton observatory.[28] The quadrupole anisotropy $\langle \sin^2 b\rangle$ is then essentially independent of the parameters, and in the range of most interest it is equal to the observed value 0.32. We see that for $p = 3\%$ and $1\% < p_n < 20\%$, i.e., for a reasonable number of neutron stars relative to the total number of stars in the Galaxy, $\langle V/V_{\max}\rangle$ and $\langle \cos\theta\rangle$ actually agree with the measured values (49). For $p = 5\%$, the region consistent with the observed values is much more tightly constrained.

We stress that Eq. (48) and the results represented in Figs. 6 and 7 actually make it possible to determine the luminosity L and energy release Q required to account for the observed isotropy. In fact, Figs. 6 and 7 show that the neutron star luminosities must lie in the narrow range

$$8 \cdot 10^{41} \text{ erg/sec} < L < 3 \cdot 10^{42} \text{ erg/sec}. \qquad (50)$$

Accordingly, the total energy release at the time of an explosion must be

$$Q \approx 10^{42}\text{–}10^{43} \text{ erg}. \qquad (51)$$

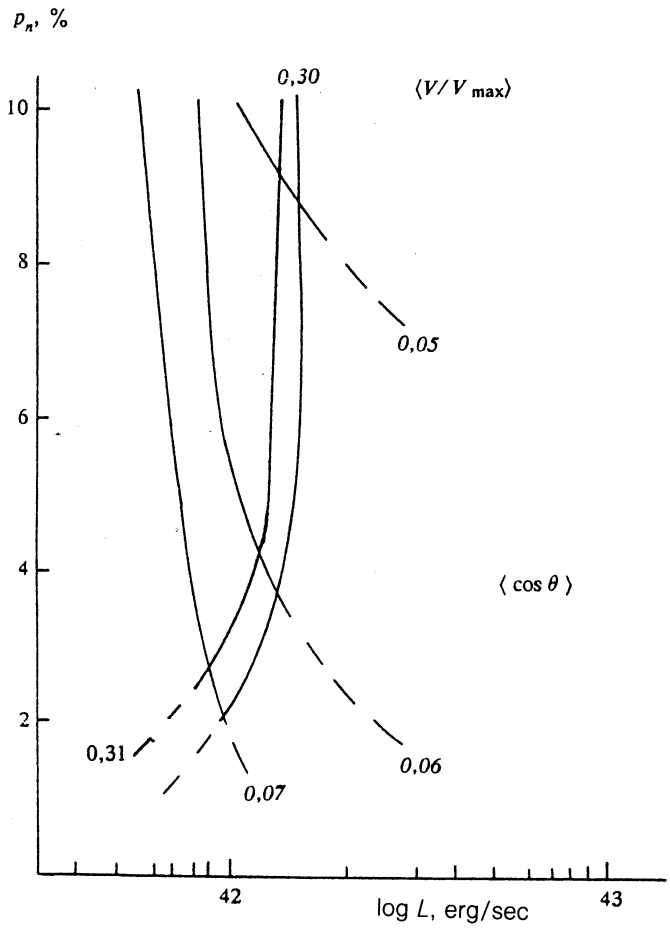

FIG. 7. Same as Fig. 6 for $p = 5\%$.

Curiously enough, this is just the luminosity the well-known repeater in the Goldfish would have if it were actually in the Large Magellanic Cloud.[1] Furthermore, we see that the width of the source distribution in luminosity L cannot be large, and it should not be more than one order of magnitude.

Finally, knowing the observed frequency of gamma ray bursts, $\nu_{\text{obs}} \simeq 800$ yr^{-1}, and the total number of observable neutron stars, $N \simeq p_n N_G \sim 2 \cdot 10^{10}$, we can estimate the repetition rate for bursts from any neutron star,

$$\nu = \nu_{\text{obs}}/N \sim 4 \cdot 10^{-8} \text{ yr}^{-1}. \qquad (52)$$

Consequently, to yield the observed burst rate, any given neutron star ought to undergo a burst with energy $Q \sim 10^{42}$–10^{43} erg [given by (51)] every 10–40 million years, on average. It is therefore no surprise that virtually no repeaters have been recorded in 20 years' observations. Moreover, Eq. (52) suggests that any neutron star in the halo ought to erupt perhaps $n_r = \nu t_G \sim 10^3$ times over the course of its lifetime ($t_G \sim 10$ billion years), so that the total gamma-ray energy liberated should be $Q_{\text{tot}} = n_r Q \sim 10^{45}$–$10^{46}$ erg. Energy losses at that high a level significantly constrain proposed gamma ray burst production mechanisms. A detailed discussion of that problem, however, lies outside our present scope.

We point out in conclusion that this theory prescribes a perfectly clear test path for the proposed model, one that is even presently feasible. As sensitivity S_{min} improves (and the radius R_{max} of the observable region increases), there should be a significant rise in source anisotropy, as indicated by Fig. 5.[1)]

Finally, we point out that above we considered a halo of dark matter—and consequently a halo of fossil neutron stars—solely for a free Galaxy. In actuality, the Milky Way is bound to M 31, the Andromeda galaxy, which is 700 kpc away. This means that at distances $r > 300$–400 kpc, the FNS halo may be distorted by the gravitational interaction between the galaxies. This may show up, in particular, in the observed isotropy of the sources. We see from Eq. (43) that neutron stars in M 31 itself are undetectable at present sensitivity levels. Anisotropy associated with the Magellanic clouds may be detectable at present sensitivities, but as yet we lack sufficient data to draw any conclusions.

It seems, then, that the rise in anisotropy of $\langle \cos\theta \rangle$ and $\langle \sin^2 b \rangle$ shown in Fig. 5 should provide an adequate test of the present model. If the anisotropy does not rise as the threshold luminosity S_{min} decreases, we will have confirmed that neutron stars in the Milky Way are not the sources of gamma ray bursts.

We thank V. L. Ginzburg for his interest and for useful discussions. We also thank E. V. Glushkov for fruitful discussions, and the referee for valuable comments.

[1)]Note that the long-dash curve in Fig. 5, which was obtained by cutting off the FNS density at $r < r_c = 20$ kpc, yields a more gradual rise in angular anisotropy.

[1]E. P. Mazets and S. V. Golenetskii, in *Astrophysics and Space Physics* [in Russian], R. A. Syunyaev (ed.), Nauka, Moscow (1982), p. 216.
[2]J. C. Higton and R. E. Lingenfelter, Ann. Rev. Astron. Astrophys. **28**, 401 (1990).
[3]A. K. Harding, Phys. Rep. **206**, 327 (1991).
[4]J.-L. Atteia, C. Barat, A. Chernenko *et al.*, Planet. Space Sci. **39**, 23 (1991).
[5]P. N. Bhat, G. J. Fishman, C. A. Meegan *et al.*, Nature **359**, 217 (1992).
[6]E. P. Mazets, S. V. Golenetskii, V. N. Il'inskii *et al.*, Astrophys. Space Sci. **80**, 1 (1981).
[7]T. Murakami, M. Fujii, K. Hayashida *et al.*, Nature **335**, 234 (1988).
[8]E. P. Liang, Astrophys. J. **304**, 682 (1986).
[9]J. J. Brainerd, Nature **355**, 132 (1992).
[10]S. Mao and B. Paczynski, Astrophys. J. **389**, L13 (1992).
[11]I. S. Shklovskii and I. G. Mitrofanov, Mon. Not. R. Astron. Soc. **212**, 545 (1985).
[12]B. Paczynski, Astrophys. J. **348**, 485 (1990).
[13]D. Hartman, R. I. Epstein, and S. E. Woosley, Astrophys. J. **348**, 625 (1990).
[14]Z. Frei, X. Huang, and B. Paczynski, Astrophys. J. **384**, 105 (1992).
[15]L. S. Marochnik and A. A. Suchkov, *Galaxies* [in Russian], Nauka, Moscow (1984).
[16]V. S. Imshennik and D. I. Nadezhin, in *Contemporary Problems in Stellar Physics and Evolution* [in Russian], A. G. Masevich (ed.), Nauka, Moscow (1989), p. 224.
[17]A. V. Gurevich and K. P. Zybin, Zh. Eksp. Teor. Fiz. **94**(10), 5 (1988) [Sov. Phys. JETP **67**, 1957 (1988)].
[18]L. D. Landau and E. M. Lifshitz, *Mechanics*, Nauka, Moscow (1973) [Pergamon Press, New York (1976)].
[19]R. A. Flores, Phys. Lett. **B215**, 73 (1988).
[20]A. V. Gurevich and K. P. Zybin, Zh. Eksp. Teor. Fiz. **97**, 20 (1990) [Sov. Phys. JETP **70**, 10 (1990)].
[21]R. N. Manchester and J. H. Taylor, *Pulsars*, Freeman, San Francisco (1977).
[22]A. G. Lyne and F. Graham-Smith, *Pulsar Astronomy*, Cambridge Univ. Press, Cambridge (1990).
[23]P. A. Harrison, A. G. Lyne, and B. Anderson, Jodrell Bank Preprint NCP 9/91 (1991).
[24]J. M. Cordes, Astrophys. J. **311**, 183 (1986).
[25]A. V. Pynzar', Astron. Zh. **70** (1993) (in press).
[26]M. E. Prokhorov and K. A. Postnov, Astron. Astrophys. Trans. **3** (1993) (in press).
[27]J. C. Higton and M. Schmidt, Astrophys. J. **355**, 13 (1990).
[28]P. N. Bhat, G. J. Fishman, C. A. Meegan *et al.*, Nature **359**, 217 (1992).
[29]C. A. Meegan, G. J. Fishman, R. B. Wilson *et al.*, Nature **355**, 143 (1992).

Translated by Marc Damashek